

Sea surface temperature in the north tropical Atlantic as a trigger for El Niño/Southern Oscillation events

Yoo-Geun Ham^{1,2}, Jong-Seong Kug^{3*}, Jong-Yeon Park³ and Fei-Fei Jin⁴

El Niño events, the warm phase of the El Niño/Southern Oscillation (ENSO), are known to affect other tropical ocean basins through teleconnections. Conversely, mounting evidence suggests that temperature variability in the Atlantic Ocean may also influence ENSO variability^{1–5}. Here we use reanalysis data and general circulation models to show that sea surface temperature anomalies in the north tropical Atlantic during the boreal spring can serve as a trigger for ENSO events. We identify a subtropical teleconnection in which spring warming in the north tropical Atlantic can induce a low-level cyclonic atmospheric flow over the eastern Pacific Ocean that in turn produces a low-level anticyclonic flow over the western Pacific during the following months. This flow generates easterly winds over the western equatorial Pacific that cool the equatorial Pacific and may trigger a La Niña event the following winter. In addition, El Niño events led by cold anomalies in the north tropical Atlantic tend to be warm-pool El Niño events, with a centre of action located in the central Pacific^{6,7}, rather than canonical El Niño events. We suggest that the identification of temperature anomalies in the north tropical Atlantic could help to forecast the development of different types of El Niño event.

The anomalous sea surface warming in the tropical Pacific during the El Niño is known to produce robust teleconnections over the tropical ocean basins. It is generally agreed that the ENSO over the Pacific domain influences Atlantic climate variability with a few months' lag^{8–11}. In particular, this remote ENSO impact on the tropical Atlantic is robust in the north tropical Atlantic (NTA) over the northern subtropics. On the other hand, ENSO is not statistically relevant to the simultaneous equatorial Atlantic variability, because the atmospheric bridge mechanism is cancelled by the opposite influence of oceanic processes¹².

Significant sea surface temperature (SST) anomalies over the NTA region are known to have broad impacts on climate variability over the US and Africa^{13–15}, and even interact remotely with North Atlantic climate^{16,17}. In addition, recent studies suggested that the Atlantic Ocean variability can influence the ENSO variability and its predictability^{1–5}. In particular, some studies argued that the equatorial Atlantic zonal mode (that is, Atlantic Niño) in boreal summer can affect ENSO development by modulating the Walker Circulation^{4,5}. Thus, it is also possible that the NTA SST may modulate the Pacific climate variability. In particular, the NTA SST can play a role in triggering ENSO events because the NTA SST has strong variability during boreal spring when the onset of most ENSO events occurs.

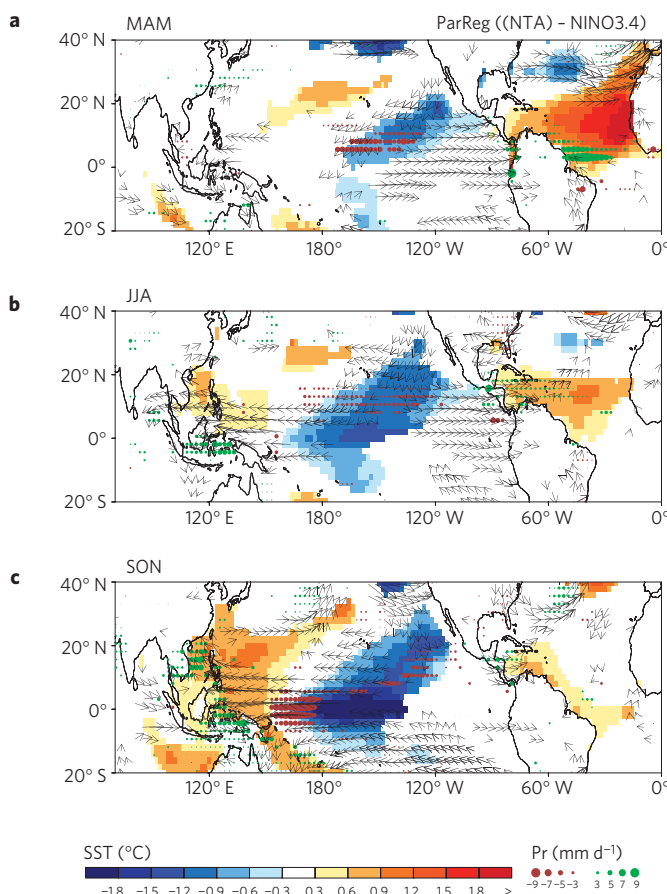


Figure 1 | Regression with respect to NTA SST. a–c, Lagged regressions between NTA SST (90°–20° E, 0°–15° N) averaged during February to April (the FMA season) and SST, wind vector at 850 hpa (vector) and precipitation during the MAM (a), JJA (b) and SON (c) seasons, after excluding the impact of NINO3.4 SST (170°–120° W, 5° S–5° N) during the previous DJF season. Only the values at the 95% confidence level or higher are shown.

To isolate the impact of NTA SST on the Pacific climate variability, lagged regressions are calculated with respect to the NTA SST (90°–20° E, 0°–15° N) during February–April (the FMA season). As it is known that the NTA SST is influenced in part by

¹Global Modeling and Assimilation Office, NASA/GSFC, Greenbelt, Maryland 20771, USA, ²Goddard Earth Sciences Technology and Research Studies and Investigations, Universities Space Research Association, Columbia, Maryland 21044, USA, ³Korea Institute of Ocean Science and Technology, Ansan 426-744, Korea, ⁴Department of Meteorology, University of Hawaii, Honolulu 96822, USA. *e-mail: jskug@kiost.ac.

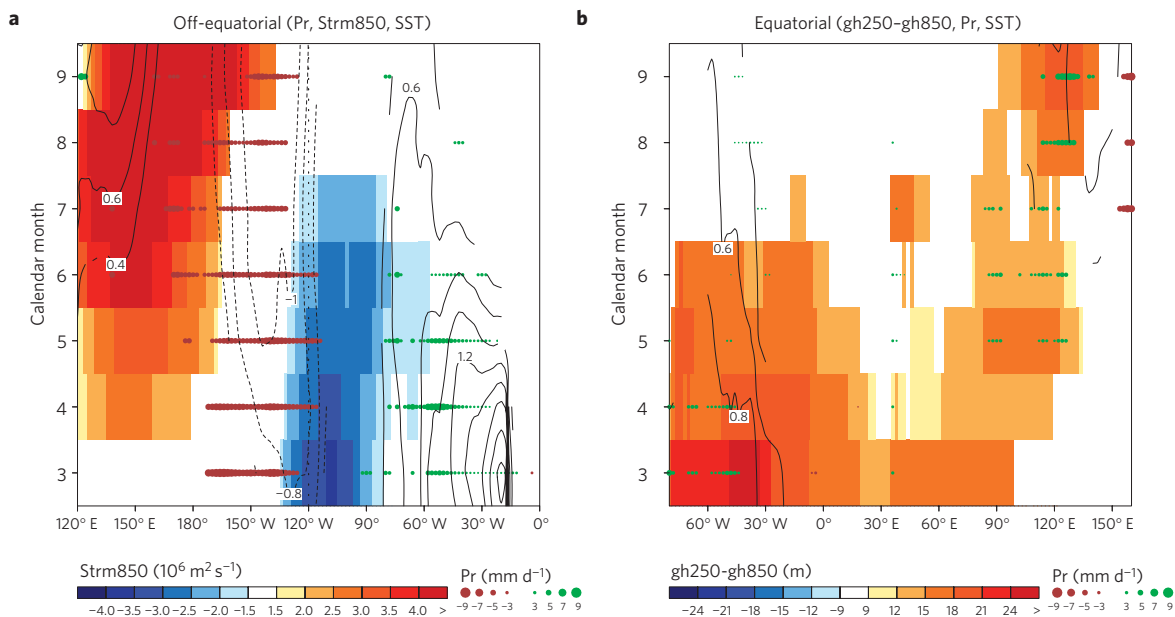


Figure 2 | Two pathways for relaying Atlantic signals to the Pacific. a, b, Lagged regressions of 3-month-averaged subtropical precipitation, stream function at 850 hPa and SST (**a**), and equatorial (10° S–10° N) thickness (that is, geopotential height at 250 hPa minus geopotential height at 850 hPa), precipitation and SST (**b**) from March to September. Note that the subtropical region of precipitation is 5°–15° N, whereas the region for other variables is 5°–20° N. Only the values with at least 95% confidence level are shown.

the ENSO variability^{10,11}, the ENSO effect is first removed using the linear regression with respect to the NINO3.4 SST (170°–120° W, 5° S–5° N) during the previous season (December–February, DJF) and then the lagged regression is obtained.

During boreal spring (the MAM season; Fig. 1a), there is a significant positive SST over the NTA region. This SST anomaly enhances the convective activity, especially over the equatorial Atlantic where the Atlantic Intertropical Convergence Zone (ITCZ) is located. The associated diabatic heating gives rise to a low-level cyclonic flow over the subtropical eastern Pacific as a Gill-type Rossby-wave response¹⁸, which produces a northerly flow on its west flank. The northerly flow leads to surface cooling through the enhanced wind speed¹⁹ and cold/dry advection from higher latitudes²⁰, resulting in an anomalous sinking motion. The associated suppression in convection is clear over the off-equatorial region in the vicinity of the ITCZ, where climatological convective activity is strong.

During boreal summer (the JJA season), the negative precipitation anomaly over the subtropical Pacific is slightly shifted to the north owing to the northward migration of the ITCZ. At the same time, the negative precipitation anomalies induce a low-level anticyclonic flow anomaly, generating a pair of circulation anomalies along the Pacific ITCZ. This anticyclonic flow enhances the northerly flow at its eastern edge, which reinforces the negative precipitation anomaly. This strong coupling among negative precipitation, the northerly flow and negative SST anomalies leads to a slow westward extension of the negative precipitation anomaly and the anticyclonic flow, which amplifies and relays the influence of the Atlantic to the Pacific. This subtropical anticyclonic flow is located over the western North Pacific, so it induces equatorial easterly anomalies over the western Pacific. This equatorial western Pacific easterly flow acts as an efficient trigger for a cold event over the equatorial Pacific by shoaling the equatorial thermocline and inducing westward zonal current anomalies²¹.

The subtropical variability in the Pacific is known to be capable of exciting an equatorial ENSO signal²², and our results demonstrate that the NTA SST is partly responsible for this subtropical signal. It is worth pointing out that there is a region of

anomalous westerly flow over the far-eastern Pacific, which is part of the NTA-forced cyclonic flow. It prevents the eastern Pacific SST from being cooled by suppressing local upwelling, thus allowing the SST anomaly to develop mainly over the central Pacific. Once the negative SST is generated over the equatorial central Pacific, it is intensified through air–sea coupled processes and leads to strong cooling during the subsequent season (Fig. 1c). During this season, the robust equatorial cold SST signal locks the negative precipitation maximum over the Equator, whereas the subtropical signals are much weakened as the ITCZ migrates southwards.

So far, it has been shown that the NTA SST warming (cooling) can initiate equatorial Pacific cooling (warming) through a pair of low-level circulation responses along the Pacific ITCZ. Figure 2 clearly illustrates the sequential evolution of this atmospheric teleconnection. Once the positive NTA SST is developed in the FMA season, the enhanced local convection generates a cyclonic flow over the eastern Pacific as a Gill-type Rossby-wave response¹⁸. Then, the anomalous convective activity, due to the anomalous northerly flow at the western part of this cyclonic flow, produces an anticyclonic flow over the western–central Pacific in the AMJ season. As this anticyclonic flow is gradually intensified through air–sea feedback, it leads to an equatorial easterly flow over the western Pacific that initiates surface cooling over the equatorial central Pacific. This westward relay of the Atlantic signal takes place along the Pacific ITCZ through the strong coupling with the wind-driven convection anomalies.

In addition to this subtropical teleconnection, the NTA SST can modulate western Pacific wind through eastward-propagating signals. During March, there is a quick response of the atmospheric thickness anomaly from the Atlantic to the eastern Indian Ocean, which might be explained by the warm Kelvin-wave response to the equatorial diabatic heating (Fig. 2b). This positive thickness signal over the eastern Indian Ocean propagates eastwards slowly, possibly owing to a coupling with the convection. This warm thickness signal is linked to a low-level low-pressure anomaly, leading to an equatorial low-level easterly flow in the region of negative zonal pressure gradient. This easterly flow induces low-level convergence over the maritime continent and

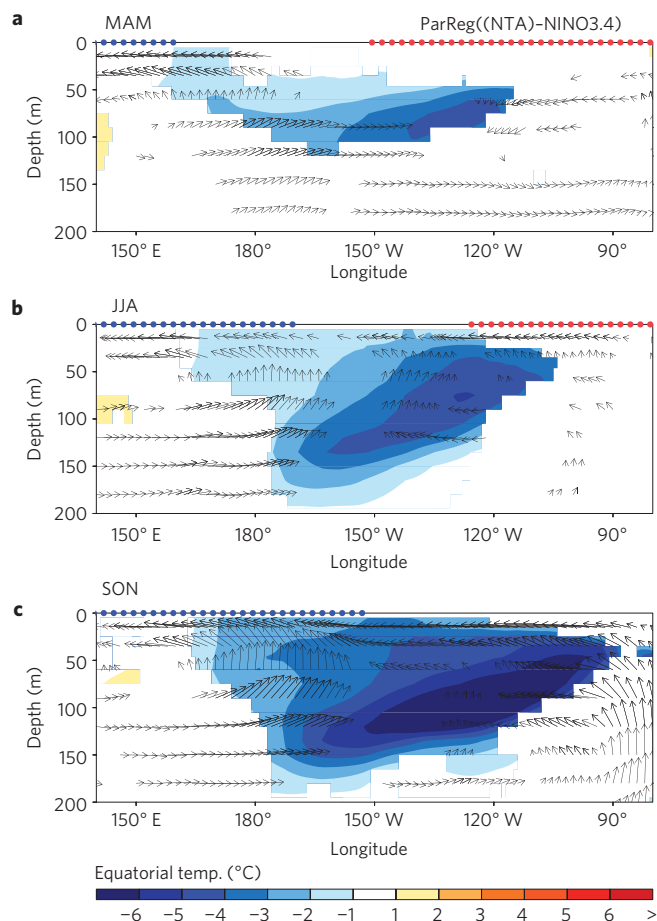


Figure 3 | Evolution of the oceanic variables with respect to NTA SST. **a–c**, Lagged regressions of equatorial (2° S–2° N) subsurface temperature, oceanic zonal currents and vertical velocities during the MAM (**a**), JJA (**b**) and SON (**c**) seasons, after excluding the impact of NINO3.4 SST (170°–120° W, 5° S–5° N) during the previous DJF season. Only the values at the 95% confidence level or higher are shown. The red and blue dots at the surface layer are marked when there are positive and negative 850-hPa zonal wind anomalies at or above the 95% confidence level, respectively.

a resultant positive precipitation anomaly in the AMJ season. In turn, the positive precipitation anomaly enhances the anomalous equatorial easterly flow.

The anomalous easterlies, induced by NTA warming, give rise to significant oceanic responses along the Equator (Fig. 3). During the MAM season, there is a weak subsurface temperature anomaly in the central Pacific related to the equatorial easterly flow. The easterly forcing also induces anomalous westward currents with the upwelling over the central Pacific through the upwelling Kelvin waves. However, these upwelling Kelvin-wave signals are not extended to the eastern Pacific, and there are even weak downwelling signals due to the local westerlies (red dots in Fig. 3a) as a part of the cyclonic flow (Fig. 1a). Therefore, the subsurface temperature anomalies cannot develop further and consequently the surface cooling is suppressed in the eastern Pacific.

During boreal summer and autumn, the westward current anomaly is extended to the east with the extension of equatorial easterly forcing, thereby the surface cooling develops further over the central Pacific. On the other hand, in the eastern Pacific, the surface cooling is not significant owing to competing processes between local westerly flow and remote easterly forcing. Therefore, the SST anomalies develop mainly over the central Pacific, rather than over the eastern Pacific. It is also noted that the temperature anomaly over the surface layer is co-located with the westward current anomaly, whereas the location of the surface anomaly is shifted to the west of the subsurface temperature anomaly, implying that the negative SST over the central Pacific is mainly driven by zonal advection⁷.

It is shown that the NTA warming in boreal spring can trigger a cold event in the subsequent winter by inducing western Pacific easterlies through both equatorial and off-equatorial pathways. As some ENSO events accompany the NTA SST events^{10,11}, our study also suggests that there is two-way feedback between ENSO and NTA SST, which leads to fast phase transition of ENSO (ref. 1 and Supplementary Fig. S9). That is, when the El Niño events accompany the NTA warming, the NTA warming can lead to fast termination of El Niño and possibly rapid development of La Niña in the subsequent winter. This implies that the NTA SST plays a critical role in modulating ENSO evolution such as its onset, and phase transition.

Even though the observational analysis clearly emphasizes the role of NTA SST on the ENSO, it has limitations due to the relatively

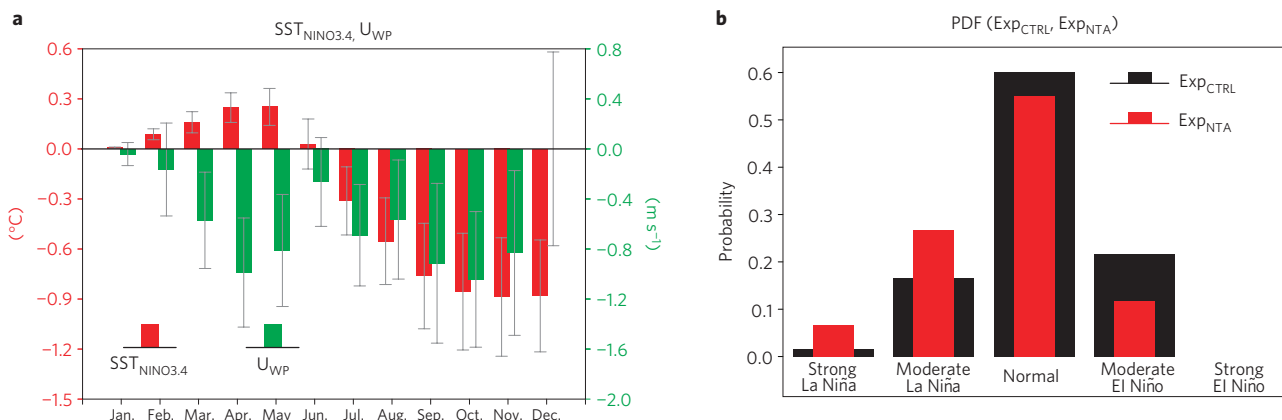


Figure 4 | The impact of the NTA SST in the idealized experiment using a CGCM. **a**, Ensemble-mean difference in the 850-hPa zonal wind over the western Pacific (120°–160° E, 5° S–5° N) and NINO3.4 SST from January to December between two CGCM simulations with and without NTA warming. Error bars indicate the 95% confidence intervals. **b**, Probability distribution of NINO3.4 SST in December using 60 ensemble simulations with the climatological SST (black bar) or with the NTA warming (red bar). Note that the moderate (strong) case is defined as the magnitude of NINO3.4 SST being between one and two (two and three) standard deviations of the 60 ensemble members.

short records with a mixture of various climate variabilities. Therefore, this observed role of the NTA SST is substantiated by idealized experiments using a coupled general circulation model (CGCM). To isolate the impact of NTA warming, two CGCM experiments are carried out with and without positive NTA SST anomalies (Supplementary Fig. S3). The differences between the two experiments are clearly due to the NTA SST, because the only difference in the experimental designs is the existence of the NTA SST anomaly.

The model results confirm that the NTA warming leads to the development of La Niña during the subsequent winter season (Fig. 4a). It is clear that the equatorial easterly anomalies are significant over the western Pacific during boreal spring, even though the equatorial Pacific SST signals are positive. This indicates that this anomalous easterly flow is induced by the NTA SST rather than by the Pacific SST. Owing to these equatorial anomalous easterlies, the La Niña signal begins to show up from boreal summer, and further develops during subsequent seasons. Note that the anomalous easterlies are weakened during boreal summer as the impact of the NTA warming is weakened, but they are reinforced during SON as the La Niña signal becomes stronger.

As in these processes, the model tends to predict that the La Niña state is more probable in 60 ensemble runs under the NTA warming (Fig. 4b). The probability of La Niña is increased 1.9 times in the simulations with the NTA warming, and the probability of having a strong La Niña is even higher ($\times 4$). On the other hand, the probability of El Niño is reduced to 52% with the NTA warming, which clearly shows that the NTA warming during spring time favours La Niña signals nine months later.

The key distinctive role of NTA SST is characterized by the opposite low-level wind responses between the western and eastern Pacific. In the case of NTA cooling, there is a region of equatorial westerly flow over the western Pacific, whereas the equatorial easterly flow is over the eastern Pacific. Therefore, surface warming prevails in the central Pacific, whereas the eastern Pacific SST does not, owing to the opposite effect of the anomalous local easterly flow. This suggests that the NTA cooling favours the development of an El Niño event whose action centre is over the central Pacific, rather than the eastern Pacific. In other words, the NTA cooling tends to be closely related to the development of the warm-pool El Niño^{6,7,23,24} (Supplementary Fig. S8 for model results), which has occurred frequently in the recent decades²⁵. Interestingly, the triggering role of NTA SST seems to be much stronger in the recent decades when the warm-pool El Niño events are frequently observed. With the increasing scientific and socioeconomic interest in the warm-pool El Niño due to its distinctive global impacts^{6,25}, a better understanding of NTA SST's role may provide a unique, and more reliable predictor for the different types of El Niño event.

Methods

In Figs 1–3, lagged regressions onto NTA SST during the FMA season are applied, after removing the regressed fields, onto NINO3.4 during the previous DJF season. This is equivalent to the partial regression method²⁶, which is often used to calculate the linearly fitted equation between two variables after excluding the linear impact of the third variable. As it captures only a linear relationship, this regression analysis has a limitation, namely, it does not reflect the asymmetry between the NTA warming and cooling events. The significance test used in this study is a two-tailed *t*-test based on the temporal standard deviation for which the distribution of the test statistics under the null hypothesis can be approximated by a *t*-distribution.

The monthly mean wind, geopotential height and precipitation from 1980 to 2010 are obtained from the Modern-Era Retrospective Analysis for Research and Applications (MERRA, <http://disc.sci.gsfc.nasa.gov/daac-bin/DataHoldings.pl>)²⁷. The observed SST data during 1980–2010 are from the improved Extended Reconstructed Sea Surface Temperature version 2 (ERSST V.2, <http://www.ncdc.noaa.gov/oa/climate/research/sst/sst.html>) from the National Climate Data Center of the US (ref. 28). In addition, the monthly mean subsurface temperature, oceanic current and vertical velocity from 1980 to 2010 are

obtained from the NCEP Global Ocean Data Assimilation System (GODAS, <http://www.esrl.noaa.gov/psd/data/gridded/data.godas.html>)²⁹. All of the data are de-trended first.

The GFDL CM2.1 model is used for the idealized CGCM experiment, which is developed by the Geophysical Fluid Dynamics Laboratory³⁰. To isolate the impact of NTA warming, two CGCM experiments are carried out by prescribing different SST fields; one is using warm NTA SST anomalies added to the observed climatological field (Exp_{NTA}, see Supplementary Fig. S3 for the prescribed SST anomalies), and the other is the control experiment of prescribing the observed climatological SST (Exp_{CTRL}). The SST fields are prescribed only over the Atlantic Ocean (5° S–25° N) in both NTA and CTRL experiments, whereas the model is fully coupled over the other regions. For the prescribed SST of the NTA warming case, the observed SST anomalies from the NTA developing season (that is, January) to the subsequent winter season (that is, December) are obtained using lag composite analysis when positive NTA SST during the FMA season is larger than one standard deviation (Supplementary Fig. S1), and then these composited SST anomalies are added to the climatological SST. A total of 60 ensemble members with different initial conditions are conducted, which are used for both the Exp_{NTA} and the Exp_{CTRL}. The *t*-test to determine the significance of ensemble-mean differences between two experiments is based on the standard deviation of differences in two experiments of each ensemble member.

Received 8 May 2012; accepted 27 November 2012;
published online 6 January 2013

References

1. Dommenges, D., Semenov, V. & Latif, M. Impacts of the tropical Indian and Atlantic Oceans on ENSO. *Geophys. Res. Lett.* **33**, L11701 (2006).
2. Jansen, M. F., Dommenges, D. & Keenlyside, N. S. Tropical atmosphere–ocean interactions in a conceptual framework. *J. Clim.* **22**, 550–567 (2009).
3. Frauen, C. & Dommenges, D. Influences of the tropical Indian and Atlantic Oceans on the predictability of ENSO. *Geophys. Res. Lett.* **39**, L02706 (2012).
4. Rodriguez-Fonseca, B. *et al.* Are Atlantic Niños enhancing Pacific ENSO events in recent decades? *Geophys. Res. Lett.* **36**, L20705 (2009).
5. Ding, H., Keenlyside, N. S. & Latif, M. Impact of the Equatorial Atlantic on the El Niño Southern oscillation. *Clim. Dynam.* **38**, 1965–1972 (2012).
6. Ashok, K., Behera, S. K., Rao, S. A., Weng, H. & Yamagata, T. El Niño Modoki and its possible teleconnection. *J. Geophys. Res.* **112**, C11007 (2007).
7. Kug, J.-S., Jin, F.-F. & An, S.-I. Two types of El Niño events: Cold tongue El Niño and warm pool El Niño. *J. Clim.* **22**, 1499–1515 (2009).
8. Enfield, D. B. & Mayer, D. A. Tropical Atlantic sea surface temperature variability and its relation to El Niño Southern Oscillation. *J. Geophys. Res.* **102**, 929–945 (1997).
9. Saravanan, R. & Chang, P. Interaction between tropical Atlantic variability and El Niño–Southern Oscillation. *J. Clim.* **13**, 2177–2194 (2000).
10. Alexander, M. A. & Scott, J. D. The influence of ENSO on air–sea interaction in the Atlantic. *Geophys. Res. Lett.* **29**, 1701 (2002).
11. Chiang, J. C. H. & Sobel, A. H. Tropical tropospheric temperature variations caused by ENSO and their influence on the remote tropical climate. *J. Clim.* **15**, 2616–2631 (2002).
12. Chang, P., Fang, Y., Saravanan, R., Ji, L. & Seidel, H. The cause of the fragile relationship between the Pacific El Niño and the Atlantic Niño. *Nature* **443**, 324–328 (2006).
13. Enfield, D. B. Relationships of inter-American rainfall to tropical Atlantic and Pacific SST variability. *Geophys. Res. Lett.* **23**, 3305–3308 (1996).
14. Chang, P., Saravanan, R., Ji, L. & Hegerl, G. C. The effect of local sea surface temperatures on atmospheric circulation over the tropical Atlantic sector. *J. Clim.* **13**, 2195–2216 (2000).
15. Wang, C., Enfield, D. B., Lee, S.-K. & Landsea, C. W. Influences of the Atlantic warm pool on Western Hemisphere Summer Rainfall and Atlantic Hurricanes. *J. Clim.* **19**, 3011–3028 (2006).
16. Watanabe, M. & Kimoto, M. Tropical–extratropical connection in the Atlantic atmosphere–ocean variability. *Geophys. Res. Lett.* **26**, 2247–2250 (1999).
17. Smith, D. M. *et al.* Skilful multi-year predictions of Atlantic hurricane frequency. *Nature Geosci.* **3**, 846–849 (2009).
18. Gill, A. E. Some simple solutions for the heat induced tropical circulation. *Quart. J. Meteorol. Soc.* **106**, 447–462 (1980).
19. Xie, S. P. A dynamic ocean–atmosphere model of the tropical Atlantic decadal variability. *J. Clim.* **12**, 64–70 (1999).
20. Ham, Y.-G., Kug, J.-S. & Kang, I.-S. Role of moist energy advection in formulating anomalous Walker Circulation associated with ENSO. *J. Geophys. Res.* **112**, D24105 (2007).
21. Kug, J.-S. & Kang, I.-S. Interactive feedback between the Indian Ocean and ENSO. *J. Clim.* **19**, 1784–1801 (2006).
22. Vimont, D. J., Wallace, J. M. & Battisti, D. S. Seasonal footprinting in the Pacific: Implications for ENSO. *J. Clim.* **16**, 2668–2675 (2003).

23. Larkin, N. K. & Harrison, D. E. On the definition of El Niño and associated seasonal average US weather anomalies. *Geophys. Res. Lett.* **32**, L13705 (2005).
24. Kao, H.-Y. & Yu, J.-Y. Contrasting eastern-Pacific and central-Pacific types of ENSO. *J. Clim.* **22**, 615–632 (2009).
25. Yeh, S.-W. *et al.* El Niño in a changing climate. *Nature* **461**, 511–514 (2009).
26. Saji, N. H. & Yamagata, T. Structure of SST and surface wind variability during Indian Ocean dipole mode events: COADS observations. *J. Clim.* **16**, 2735–2751 (2003).
27. Rienecker, M. M. *et al.* MERRA—NASA’s Modern-era retrospective analysis for research and applications. *J. Clim.* **24**, 3624–3648 (2011).
28. Smith, T. & Reynolds, R. Improved extended reconstruction of SST (1854–1997). *J. Clim.* **17**, 2466–2477 (2004).
29. Behringer, D. W. & Xue, Y. *8th Symp. on Integrated Observing and Assimilation Systems for Atmosphere, Oceans, and Land Surface, AMS 84th Annual Mtg* 11–15 (Washington State Convention and Trade Center, 2004).
30. Delworth, T. L. *et al.* GFDL’s CM2 global coupled climate models. Part I: Formulation and simulation characteristics. *J. Clim.* **19**, 634–674 (2006).

Acknowledgements

This work was supported by the National Research Foundation of Korea (Grant NRF-2009-C1AAA001-2009-0093042) funded by the Korean government (MEST), and KIOST (PE98801). F.F.J. was supported by US NSF grant ATM1034798, US Department of Energy grant DESC005110 and US NOAA grant NA10OAR4310200.

Author contributions

Y.-G.H., J.-S.K. and F.-F.J. designed the research and wrote the paper. Y.-G.H. and J.-Y.P. performed the experiments and analysed the data. All of the authors discussed the results and commented on the manuscript.

Additional information

Supplementary information is available in the [online version of the paper](#). Reprints and permissions information is available online at www.nature.com/reprints. Correspondence and requests for materials should be addressed to J.-S.K.

Competing financial interests

The authors declare no competing financial interests.